ELSEVIER

Journal of Photochemistry and Photobiology A: Chemistry 148 (2002) 233–245

Journal of Photochemistry and Photobiology A:Chemistry

www.elsevier.com/locate/jphotochem

Photocatalytic oxidation of organics in water using pure and silver-modified titanium dioxide particles

Veronica Vamathevan [a], Rose Amal [a,*], Donia Beydoun [a], Gary Low [b], Stephen McEvoy [c]

[a] Centre for Particle and Catalyst Technologies, School of Chemical Engineering and Industrial Chemistry, The University of New South Wales, UNSW, Sydney, NSW 2052, Australia
[b] NSW Environment Protection Authority, Environmental Chemistry Section, Environmental Science Branch, Lidcombe, NSW 2141, Australia
[c] CSIRO Energy Technology, Lucas Heights Science and Technology Centre, Lucas Heights, NSW 2234, Australia

Received 24 July 2001; received in revised form 25 September 2001; accepted 25 September 2001

Abstract

The simultaneous photocatalytic degradation of organic compounds and reduction of silver ions in titanium dioxide suspensions at pH 3.0–3.5 has been studied. The organic compounds of interest were sucrose and salicylic acid.

The presence of silver ions in TiO_2 suspensions was found to enhance the photooxidation of high loadings (2000 μg C) of sucrose. However, for low sucrose loadings (100 μg C), pure TiO_2 particles performed as well as modified TiO_2 particles. An optimum silver ion loading of 2.0 at.% Ag^+ was observed for the mineralisation of 2000 μg C sucrose. At this silver ion loading, the mineralisation of 2000 μg C sucrose was enhanced by a factor of approximately 4.0 (based on 90% overall oxidation rates). In contrast, the addition of silver ions to TiO_2 suspensions did not have any significant effect on the photocatalytic mineralisation of salicylic acid to carbon dioxide, for both low and high loadings of salicylic acid in the suspension. It was also observed that pure TiO_2 particles performed as well as silver-modified TiO_2 particles for the degradation of 2000 μg C salicylic acid.

The higher activity of silver ion-modified titanium dioxide suspensions for sucrose mineralisation is predominantly due to the presence of small silver particles on the titania surface, rather than due to the trapping of electrons during the reduction of silver ions. Approximately 50% of the initial mass of silver ions added to TiO_2 suspensions were reduced to metallic silver deposits in the presence of sucrose and salicylic acid mineralisation at the 2.0 at.% Ag^+ loading.

Nanosize silver deposits on TiO_2 particles act as sites of electron accumulation where the reduction of adsorbed species such as oxygen occur. The enhanced reduction of oxygen through better electron–hole separation in Ag/TiO_2 particles compared to pure TiO_2 particles increases the rate of sucrose mineralisation. Therefore, it is proposed that the rate-limiting step in the sucrose photooxidation reaction is the transfer of electrons to dissolved oxygen molecules, whereas in the case of salicylic acid degradation and mineralisation, the rate-limiting step is the attack of salicylic acid molecules and its degradation intermediate products by holes and hydroxyl radicals. Hence silver deposits on TiO_2 particles are not beneficial for the photocatalytic degradation and mineralisation of salicylic acid but are advantageous for the mineralisation of sucrose.

Keywords: Photocatalysis; Silver ion; Titanium dioxide; Sucrose; Salicylic acid

---

1. Introduction

The use of heterogeneous photocatalysis for the non-selective destruction of organic and inorganic waste materials has been widely demonstrated in numerous laboratory studies. Organic compounds such as chlorinated alkanes and alkenes, polychlorinated phenols, aromatics, aldehydes, organic acids and amines can be oxidised to carbon dioxide, water and mineral acids using near-UV or solar illuminated TiO_2 particles [1]. The photocatalytic reduction of disulphides to the corresponding thiols has been successfully performed [2], as well as the reduction of metal ions such as Ag^+ [3–8], Pt^{4+} [3,8–10], Pd^{2+} [11,12], Au^{3+} [13,14], and Ni^{2+} [15]. These metal ions have reduction potentials that are more positive than the conduction band edges of common semiconductors. Metal cations whose potentials do not permit their reduction can be oxidised and deposited on the semiconductor as insoluble oxides [16].

When semiconductor particles (e.g. titanium dioxide, TiO_2) are illuminated with light of energy equal to or greater than the bandgap energy, electrons are excited from the valence band to the conduction band, forming positively charged holes in the valence band. Photogenerated electrons and holes participate in redox reactions with adsorbed species on the semiconductor surface such as hydroxyl

---

* Corresponding author. Tel.: +61-2-93854361; fax: +61-2-93855966.
E-mail address: r.amal@unsw.edu.au (R. Amal).

1010-6030/02/$ – see front matter
PII: S1010-6030(02)00049-7

ions, water molecules, dissolved oxygen molecules, organic species and metal ions. Alternatively holes and electrons may recombine making them unavailable to participate in useful redox reactions.

Both oxidation and reduction processes occur on the surface of the same semiconductor particle, often only separated by a distance of a few angstroms [17]. The efficiency of photocatalytic reactions is limited by the high degree of electron–hole recombination inherent in photocatalytic processes and by the limited absorption capability of photocatalysts.

Various attempts have been made to reduce electron–hole recombination in photocatalytic processes and to extend the absorption range of TiO_2 particles into the visible range. These include dye sensitisation (surface derivatisation), incorporation of metal ions into the crystalline titanium dioxide lattice, surface modification of photocatalysts by noble metal deposits [3,18] and surface chelation [19].

In this study, pure and surface-modified titanium dioxide particles were used for the photocatalytic oxidation of sucrose and salicylic acid. The objective of this study was to improve the activity of TiO_2 using surface modification and to compare the activity of the photocatalyst before and after surface modification with metallic silver deposits for the degradation and mineralisation of organics. Titania and silver/titania particles were also characterised using a number of techniques (BET, TEM). Some explanations have been made to understand the mechanism by which surface modification affects catalyst activity.

2. Experimental

2.1. Chemicals

The titanium dioxide (TiO_2) sample used in all experiments was Degussa P25 (Degussa). Suspensions of TiO_2 (0.2 wt.%) were adjusted to pH 3.0 or 3.5 prior to reaction using 0.5 M perchloric acid ($HClO_4$). Perchloric acid (70 wt.%, analytical grade) was obtained from Aldrich Chemical. Modified TiO_2 suspensions were prepared by adding the required quantities of silver(I) nitrate ($AgNO_3$) to the suspension such that the desired Ag/Ti atom ratio was obtained. Silver nitrate (99.9999 wt.%, analytical grade) was purchased from Aldrich Chemical. The activities of bare and modified photocatalysts were compared based on the photocatalytic oxidation of sucrose and salicylic acid in water. Sucrose was supplied by Fisons Scientific Equipment and salicylic acid (+99% pure) was purchased from Aldrich Chemical. MilliQ water purified by a Millipore unit (Milli-Q PLUS) was used in the preparation of all suspensions and solutions.

2.2. Photocatalytic Activity Studies

Photocatalytic reactions were performed in a slurry-type batch reactor. The apparatus and analysis procedure used in this work are similar to that previously described by Abdullah et al., 1990 [20]. The reactor consists of two glass coils of similar height mounted vertically on a metal board. The coils were constructed using borosilicate tubing (5.0 mm inside diameter, 6.0 mm outside diameter). A blacklight fluorescent lamp (NEC, 15W, maximum emission at ~350 nm, emission range 300–400 nm) mounted on a domestic lamp holder, was fitted through the centre of each coil. The glass coils are connected to a gas–liquid separator, a conductivity cell ($K = 0.1\,\mathrm{cm}^{-1}$) and a peristaltic pump (Masterflex® Quick Load, Cole Parmer Instrument, Extech Equipment) by means of Viton flexible tubing. The gas–liquid separator and the conductivity cell are also made of borosilicate glass.

The TiO_2 slurry (20 ml) and organic solution are introduced into the system at the loading port of the gas–liquid separator. The mineralisation of sucrose and salicylic acid were followed by measuring the amount of carbon dioxide generated as a function of time. The gas ($CO_2 + \mathrm{air}$)–liquid mixture is circulated through the loop by the pump. Rapid intermingling of the gas and liquid phases in the spiral ensures that carbon dioxide equilibration is quickly established [21]. Separation of the gas and liquid phases occurs in the gas–liquid separator. The gas phase passes through the conductivity cell before returning to the reaction mixture. The conductivity cell consists of a probe dipped in 10 ml of MilliQ water, having a gas inlet at the bottom and an air outlet at the top. Air leaving the outlet is returned back to the circulating suspension. The conductivity was measured with an Alpha 800 conductivity meter. As increasing amounts of organic carbon are mineralised, the amount of carbon dioxide generated increases, resulting in increasing conductivity readings. The conductivity readings increase and reach a constant value when all the organic carbon is completely oxidised to CO_2. Readings were taken every 10 s.

Conductivity readings were converted to the mass of carbon generated (as carbon dioxide) by means of a calibration curve. The calibration curve was constructed using the following method. Known masses of carbon (as sucrose) (25, 50, 100, 250 μg C, etc.) were oxidised and the conductivity reading corresponding to the complete mineralisation of each carbon mass to CO_2 was recorded. A calibration curve was obtained by plotting ln(conductivity) versus ln(mass of carbon). The linearised expression derived from the calibration curve was of the form: carbon (μg) = $\exp[\{\ln(\mathrm{conductivity} - \mathrm{LF}) - \mathrm{intercept}\}/\mathrm{slope}]$, where is the conductivity (in μS/cm) and LF the linearising factor. The values obtained for the mass of carbon as CO_2 generated were normalised to account for differences in the amount of ambient carbon dioxide dissolved in water from day to day.

The desired amounts of sucrose or salicylic acid solution and silver nitrate (in the case of modification of the TiO_2 slurry with metal ions) were injected into the suspension. The mixture was circulated through the reactor for 5–15 min prior to illumination to allow adsorption of organic molecules and silver ions onto the photocatalyst surface. The simultaneous photooxidation of organic and photoreduction of silver ions were performed in the presence of air. Each experimental run was duplicated to ensure the reproducibility of the results.

2.3. Analysis techniques

2.3.1. Inductively coupled plasma-atomic emission spectroscopy

Inductively coupled plasma-atomic emission spectroscopy (ICP-AES) was used to determine the mass of silver deposited on the TiO_2 particles. An accurately weighed sample of the modified photocatalyst was digested in 5 ml of concentrated (1:1) HNO_3 on a hot plate. The digested sample was filtered (Whatman Filter 542) into a 50 ml volumetric flask and diluted to the mark with deionised water. The sample was analysed on a Perkin Elmer Optima 3000 ICP-AES instrument. Digestion and analysis of a pure TiO_2 sample was also conducted as a blank run.

2.3.2. UV–visible absorbance spectrophotometry

Absorbance spectrophotometry (Varian CARY 1E UV–visible spectrophotometer) was used to measure the concentration of salicylic acid in solution. Salicylic acid has maximum absorbance of UV–visible light at a wavelength of 294 nm. The instrument was calibrated using standards prepared in the range 0–200 ppm. A linear calibration curve was obtained for salicylic acid concentrations in the range 0–100 ppm.

2.4. Characterisation methods

2.4.1. Transmission electron microscopy (TEM)

TEM was used to investigate the size and distribution of the silver deposits on the titania surface on various modified samples. A small amount of dry powder was dispersed in ethanol by ultrasonic agitation. Two droplets of the suspension were placed on a carbon-coated copper grid and analysed under a Philips CM200 field emission gun microscope equipped with an EDAX energy dispersive X-ray spectroscopy system (EDS detector). X-ray mapping of the samples was also conducted.

2.4.2. Brunauer–Emmett–Teller surface area measurements (BET)

The surface area of titanium dioxide samples before and after modification with silver deposits was measured by nitrogen gas adsorption on the ASAP 2000 Micromeritics Philsorb and Porosimeter.

3. Results and discussion

3.1. Characterisation studies of pure TiO_2 particles and silver-modified TiO_2 particles

3.1.1. TEM

TEM enabled identification of the location, distribution and size of the silver deposits on the titania surface. Fig. 1(a) and (b) are TEM micrographs of modified TiO_2 particles (20.0 at.% Ag^+ loading). The size of the titania crystallites was unchanged as a result of surface modification by silver particles. Silver deposits were located on the surface of the individual TiO_2 crystallites. The distribution and size of the silver deposits differed as the Ag^+ ion loading was varied. At the 2.0 at.% Ag^+ loading, silver particles were approximately 5.0 nm in size while at the 20.0 at.% Ag^+ loading, Ag deposits of approximately 2.0 nm in size were observed [22]. Agglomerates of metallic silver up to 125.0 nm in size were also observed on TiO_2 particles at the 20.0 at.% Ag^+ loading (Fig. 1(a) and (b)). Herrmann et al. [6] have reported that agglomerates of silver up to 400 nm in size were present at high silver loadings (38.0 wt.%) in addition to small Ag particles.

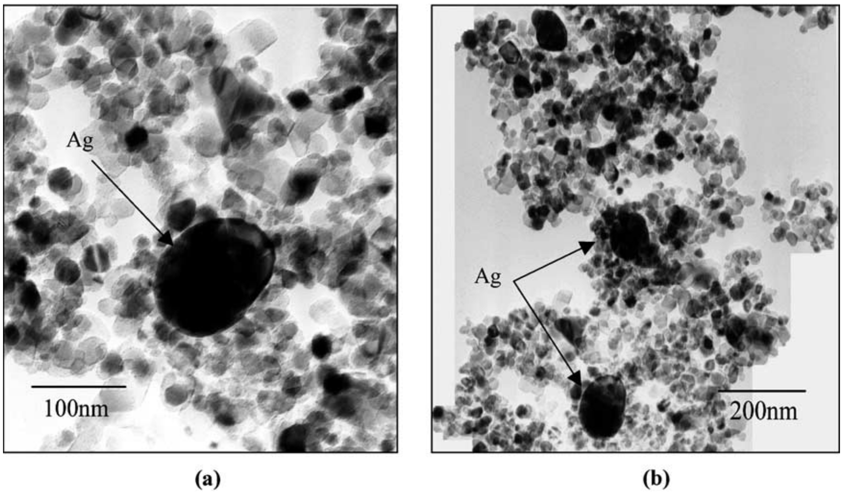

(a) (b)

Fig. 1. TEM micrographs of 20.0 at.% (a and b) Ag-modified Degussa P25 particles after use for the mineralisation of 100 μg C sucrose.

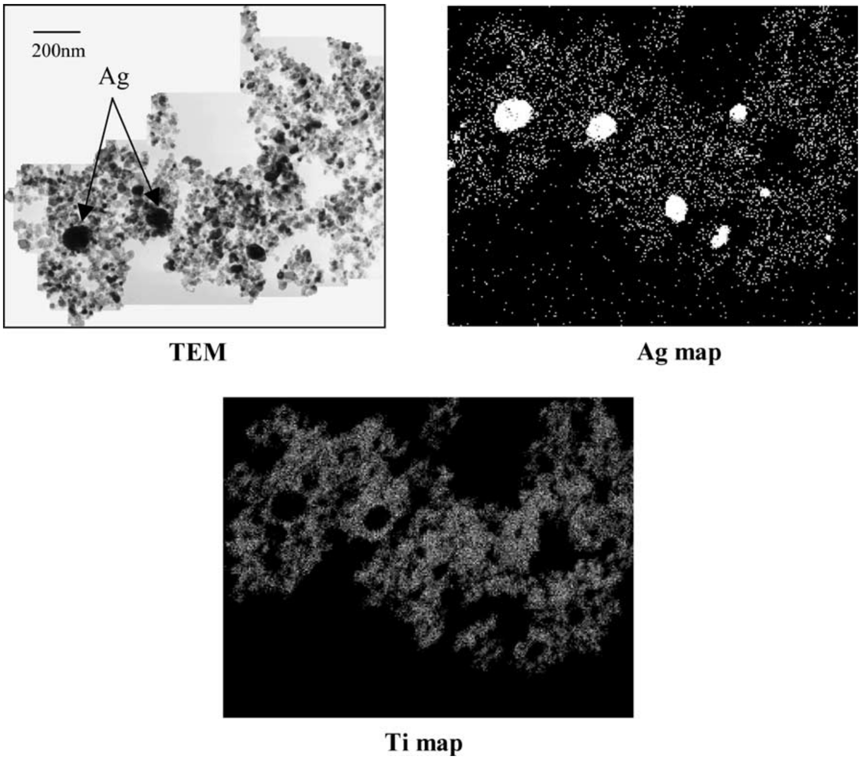

TEM

Ag map

Ti map

Fig. 2. X-ray maps of 20.0 at.% Ag-modified Degussa P25 particles after use for the mineralisation of 100 μg C sucrose.

Silver particles were not deposited on all TiO_2 particles present in the suspension at the 2.0 at.% Ag^+ loading. However, at the 20.0 at.% Ag^+ loading, silver particles covered the entire surface of all TiO_2 particles, giving the surface and edges of the particles a rough appearance [22].

X-ray maps of modified particles (at the 20.0 at.% Ag^+ loading) are shown in Fig. 2. The maps show where the silver particles are located and the extent of TiO_2 surface coverage by Ag nanoparticles. The presence of silver agglomerates on the TiO_2 particles is shown clearly. The “Ag map” shows the location of Ag particles while the “Ti map” shows the location of the TiO_2 particles.

3.1.2. BET surface area analysis

The surface area of titanium dioxide particles before and after surface modification with silver deposits was determined using nitrogen gas adsorption. The surface areas obtained are shown in Table 1. There was no significant change in the surface area after metallisation of TiO_2 particles.

3.2. Photooxidation of sucrose using bare and silver ion-modified titanium dioxide suspensions

When photocatalyst (e.g. TiO_2) particles are illuminated with light of energy equal to or greater than the bandgap energy, valence band electrons are excited into the conduction band, leaving vacant sites or holes in the valence band. Conduction band electrons and valence band holes migrate to the surface of the catalyst where they take part in a series of redox reactions, described by the following equations:

1. Electron–hole pair generation

$$TiO_2 \xrightarrow{h\nu \geq E_g} e_{cb}^- + h_{vb}^+ \tag{1}$$

2. Possible traps for holes

   (a) Surface-adsorbed hydroxyl ions

$$h_{vb}^+ + OH_{ads}^- \rightarrow OH_{ads}^\bullet \tag{2}$$

Table 1
BET surface areas of pure and silver-modified TiO_2 particles

Photocatalyst	BET surface area (m^2/g)
P25 before reaction	56.6
P25 after 2000 μg C sucrose photooxidation	56.1
2.0 at.% Ag^+/P25 after 2000 μg C sucrose photooxidation	55.4
20.0 at.% Ag^+/P25 after 2000 μg C sucrose photooxidation	51.3

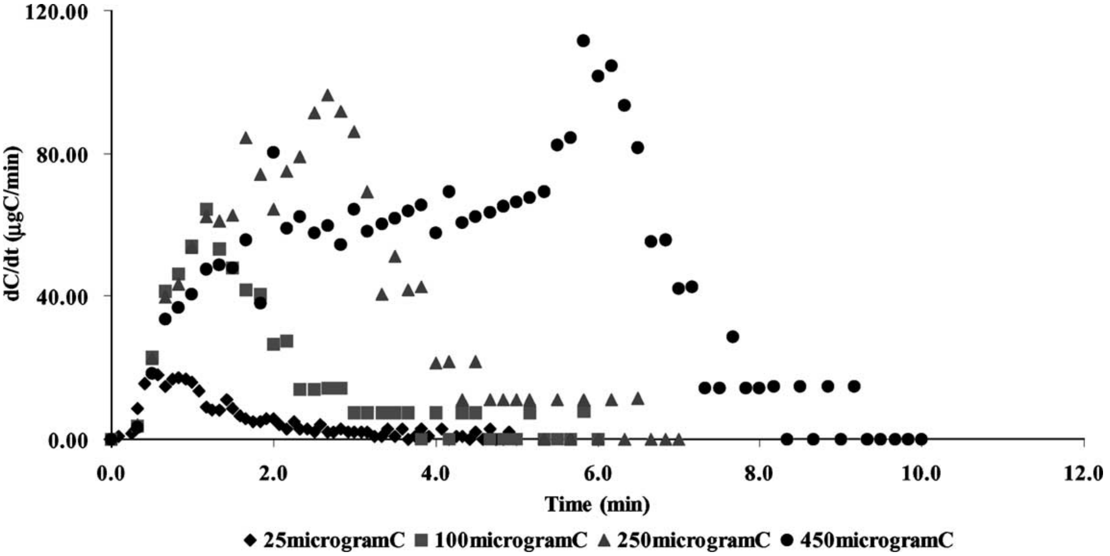

Fig. 3. Oxidation of 25, 100, 250, and 450 µg C sucrose using pure Degussa P25 suspensions at pH 3.5.

(b) Surface-adsorbed water molecules

$$h_{vb}{}^{+} + H_2O_{ads} \rightarrow OH_{ads}{}^{\bullet} + H^{+} \quad (3)$$

$$h_{vb}{}^{+} + H_2O_{ads} \rightarrow \tfrac{1}{2}O_2 + H^{+} \quad (4)$$

(c) Electron donor (D) species

$$h_{vb}{}^{+} + D_{ads} \rightarrow D_{ads}{}^{+} \quad (5)$$

3. Possible traps for electrons

(a) Surface traps (shallow traps)

$$e_{cb}{}^{-} + \mathrm{Ti(IV)OH} \rightarrow \mathrm{Ti(III)OH} \quad (6)$$

(b) Lattice traps (deep traps)

$$e_{cb}{}^{-} + \mathrm{Ti(IV)} \rightarrow \mathrm{Ti(III)} \quad (7)$$

(c) Electron acceptor (A) species

$$e_{cb}{}^{-} + A_{ads} \rightarrow A_{ads}{}^{-} \quad (8)$$

4. Recombination

$$e_{cb}{}^{-} + h_{vb}{}^{+} \rightarrow TiO_2 + \text{energy} \quad (9)$$

In bare TiO_2 suspensions, the electron donating species are water molecules, hydroxyl ions and sucrose molecules. The electron accepting species is oxygen for experiments conducted in the presence of air. In modified TiO_2 suspensions, an additional electron accepting species is introduced, namely silver(I) ions.

The photooxidation of sucrose in water was performed using bare TiO_2 particles under acidic conditions. Sucrose ($C_{12}H_{22}O_{11}$) was chosen as a model compound for this study as it is a simple compound without heteroatoms such as S, Cl, and P, which may interfere with the photooxidation rate [20,23]. The initial pH of the suspensions was adjusted to pH 3.5. Figs. 3 and 4 show the rate of change in carbon dioxide generated (in terms of carbon (C)) with respect to changes in time versus illumination time for the oxidation of various amounts of carbon (as sucrose) (dC/dt versus time). As increasing amounts of carbon are oxidised (250 µg C (12.5 ppm C), 450 µg C (22.5 ppm C), 2000 µg C (100.0 ppm C)), the shape of the oxidation profiles change indicating a sudden increase in the rate of carbon dioxide generation towards the latter part of the reaction. Changes in the pH of the suspension were not observed after irradiation.

Fig. 5 illustrates the oxidation of 2000 µg C sucrose at pH 3.5 using silver-modified TiO_2 particles. The silver ion (Ag^+) loadings added to the suspension were 0.5, 1.0, 2.0, 3.0, 5.0, 10.0 and 20.0 at.%. Silver-modified particles exhibited activities that were significantly higher than that of bare TiO_2 particles at all Ag^+ loadings. An optimum silver ion loading exists at 2.0 at.%. At the optimum Ag^+ loading in suspension, the oxidation of 2000 µg C sucrose was enhanced by a factor of approximately 4.0 (based on 90% overall oxidation rates). The 2000 µg C sucrose oxidation profiles of silver-modified TiO_2 particles do not feature a peak in the oxidation rate towards the end of the reaction as in the case of bare TiO_2 particles. Rather, there is a region of constant oxidation rate, indicating saturation of the modified TiO_2 surface with physisorbed sucrose molecules. To determine whether there was a change in the shape of the oxidation profile when using Ag-modified TiO_2 photocatalysts for even higher sucrose loadings, a 2.0 at.% Ag^+-modified TiO_2 suspension was used for the oxidation of 10,000 µg C sucrose. There was no noticeable change in the shape of the oxidation curve (dC/dt versus illumination time).

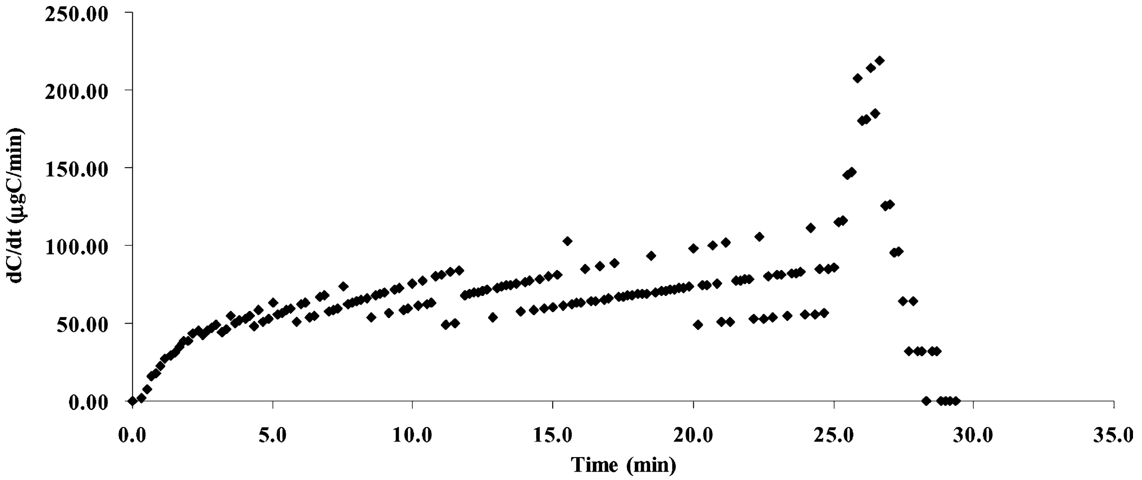

Fig. 4. Oxidation of 2000 μg C sucrose using pure Degussa P25 particles at pH 3.5.

Titanium dioxide particles in suspension changed colour during irradiation in the presence of silver ions and sucrose. At the 2.0 at.% Ag^+ loading, the particles changed from white to light brown. At the 20.0 at.% Ag^+ loading, the colour changed from white to yellow. The presence of metallic silver deposits on the titania particles was confirmed by X-ray diffraction (XRD) analysis of the particles [22].

The pH of the modified suspensions decreased during the photooxidation of sucrose, for all sucrose and Ag^+ loadings used. A similar pH decrease was observed during the photoreduction of silver ions onto titania in the absence of sucrose oxidation. Hence, the decrease in pH is attributed to silver ion reduction. The final pH of 2.0 at.% Ag^+ and 20.0 at.% Ag^+-modified suspensions after illumination were 3.2 and 2.5, respectively.

Ilisz et al. [24] observed that in the absence of phenol, the reduction of Ag^+ was accompanied by a decrease in pH and the observed (moles of formed H^+)/(moles of reduced Ag) was near the theoretical value of 1.0. The pH decrease is due to the oxidation of water by holes (Eq. (4)) [4,25,26]. The generated oxygen can be consumed during the photooxidation reaction. The mass of silver ions reduced to metallic silver as a percentage of the initial mass of silver ions added to the suspension in the presence of organic mineralisation were 46.1 and 64.8%, for the 2.0 at.% Ag^+ and 20.0 at.% Ag^+ loadings, respectively. Silver ions can also be reduced (onto the walls of the photoreactor) in the absence of photocatalyst particles but under near-UV illumination, with and without organic molecules present in the system.

The enhanced activity of titanium dioxide particles for sucrose mineralisation as a result of silver ion addition to the TiO_2 suspension can be attributed to two factors. Firstly, the reduction of silver ions to metallic silver consumes electrons. This enhances the separation of electrons and holes and reduces recombination [28]. Secondly, the metal deposits on

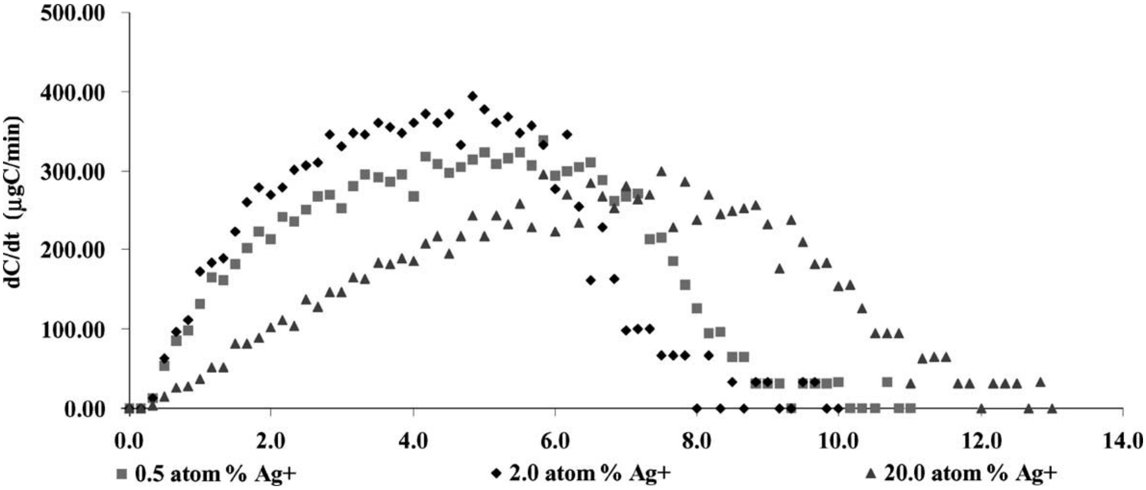

Fig. 5. Oxidation of 2000 μg C sucrose using silver ion-modified Degussa P25 suspensions at pH 3.5.

the titania surface are reported to be responsible for the improved activity of TiO_2 particles and films [5,7,28].

To distinguish whether the enhancement in sucrose mineralisation rate was due to the reduction of silver ions to silver metal, or due to presence of metallic silver particles on the TiO_2 surface, a 2.0 at.% Ag^+-modified TiO_2 suspension was used in three consecutive reactions for the oxidation of 2000 μg C sucrose, without the addition of new $AgNO_3$ into the suspension for the second and third oxidation runs [22]. The three oxidation profiles obtained were similar and indicated that the enhanced activity of the modified particles was predominantly due to the presence of deposited species on the TiO_2 surface. A small decrease in catalyst activity between the first and second oxidation runs (as indicated by the respective oxidation curves) showed that the beneficial effect of reduced electron–hole recombination due to electron-trapping by Ag^+ ions also contributes to the enhanced activity to a small extent.

The improved activity of metallised Degussa P25 particles is due to better charge separation and therefore, less recombination. Electronic interactions occur between metal deposits on the titania surface and the TiO_2 particles. If the work function of the metal is higher than that of titania (work function of $Ag = 4.73\,eV$), then electrons are removed from TiO_2 particles in the vicinity of each metal particle. This results in the formation of Schottky barriers at each metal–semiconductor contact region and results in charge separation [16].

The rate-limiting step in photocatalytic oxidations is believed to be the transfer of electrons from the TiO_2 surface to oxygen molecules. Hence, negative charging of photocatalyst particles results as hole transfer to adsorbed organics or to water occurs at a faster rate than the two-electron transfer to dioxygen. In air-equilibrated systems, as a result of the improved separation of electrons and holes, metal deposits on the TiO_2 surface enhance photocatalytic reactions by accelerating the transfer of electrons to dissolved oxygen molecules. Oxygen is a good electron acceptor and its reduction is favourable in acidic media.

The rate of e^- transfer to adsorbed O_2 depends on the density of shallow (0.1–0.3 eV) surface and near-surface electron traps. Those TiO_2 catalysts with high densities of shallow traps are likely to be the most effective in photocatalytic oxidation reactions since electrons are immobilised in surface traps before being transferred to O_2 molecules. Therefore the incorporation of group VIII metal O_2 reduction catalysts or noble metals on the photocatalyst surface should increase the rate of e^- transfer to O_2 and thereby raise the quantum yield [28]. The transfer of electrons to metal deposits, results in the deposits becoming negatively charged.

$$Ag + e^- \leftrightarrow e^-(Ag) \tag{10}$$

The superoxide radical is formed as a result of oxygen reduction by photogenerated electrons. The following equations (Eqs. (11)–(21)) describe the formation of hydroxyl radicals via the generation of hydrogen peroxide (H_2O_2) and the peroxyl radical. The generation of hydroxyl radicals is important for the oxidation of organic molecules.

$$O_{2_{ads}} + e_{cb}^- + O_2^{\bullet -} \tag{11}$$

$$O_2^{\bullet -} + H^+ \leftrightarrow HO_2^{\bullet} \tag{12}$$

$$HO_2^{\bullet} + HO_2^{\bullet} \rightarrow H_2O_2 + O_2 \tag{13}$$

$$O_2^{\bullet -} + HO_2^{\bullet} \rightarrow HO_2^- + O_2 \tag{14}$$

$$HO_2^- + H^+ \rightarrow H_2O_2 \tag{15}$$

$$O_2^{\bullet -} + H_2O_2 \rightarrow {}^{\bullet}OH + OH^- + O_2 \tag{16}$$

$$H_2O_2 + e^- \rightarrow {}^{\bullet}H_2O_2 \tag{17}$$

$$O_2^- + {}^{\bullet}H_2O_2 \rightarrow {}^{\bullet}OH + OH^- + O_2 \tag{18}$$

$$H_2O_2 + 2e^- + 2H^+ \rightarrow 2H_2O \tag{19}$$

$$H_2O_2 + 2h^+ \rightarrow H^+ + O_2 \tag{20}$$

$$H_2O_2 + h\nu \rightarrow 2{}^{\bullet}OH \tag{21}$$

Another consideration is that the superoxide radical, which itself has a relatively low oxidising capability, may combine with organoperoxy radicals ($ROO^{\bullet}$) to generate an unstable tetroxide (ROOOOH) which decomposes to the reaction products [24]:

$$HO_2^{\bullet} + ROO^{\bullet} \rightarrow ROOOOH \rightarrow\rightarrow \text{products} \tag{22}$$

Alternatively, dissolved oxygen can also react with organic radicals formed during illumination of the suspension to forming organoperoxy radicals, which are degraded further to carbon dioxide and water [24].

$$R^{\bullet} + O_2 \rightarrow ROO^{\bullet} \rightarrow\rightarrow \text{products} \tag{23}$$

The enhanced activity of silver-modified samples cannot be attributed to changes in the surface area of the samples. According to BET surface area measurements (Table 1), the surface area is hardly changed before and after surface modification, even at the highest silver loading used (20.0 at.% Ag^+).

An optimum silver ion loading of 2.0 at.% Ag^+ was found to exist for the photooxidation of 2000 μg C sucrose. For all silver ion loadings used, Ag/TiO_2 performed significantly better than bare TiO_2. Above the optimum silver ion loading, the activity of Ag/TiO_2 particles decreased. There are several reasons for the existence of an optimum metal loading. For metal loadings above the optimum, a decrease in the electron density of TiO_2 occurs due to electron attraction by the much more numerous metal particles formed with higher metal ion loadings. However, the resulting complicated field configuration has a detrimental effect on charge separation, lowering the activity of the modified photocatalyst [16]. Also, excessive coverage of the photosensitive surface by silver deposits for particles prepared with Ag^+ loadings greater than 2.0 at.% decreases the amount of light reaching the TiO_2 surface [1,29]. This reduces the number of electron–hole pairs generated and lowers the rate of organic oxidation. It is also possible that above the optimum loading, silver particles can also act as recombination centres [5]. Negatively charged silver sites begin to attract positively charged holes, thereby becoming recombination centres. There is also the increased probability for the capture of holes by the large number of silver particles at high metal loadings, which decreases the probability of holes reacting with adsorbed species at the TiO_2 surface [5]. This is related to the particle size of silver deposits. The particle size of the silver deposits is an important parameter influencing the photocatalytic activity of Ag/TiO_2 particles. Smaller deposits can trap holes faster than large deposits.

Fig. 1 shows TEM plates of the Ag/TiO_2 (20.0 at.% Ag^+) particles prepared in this work. At the 2.0 at.% Ag^+ loading, silver deposits were estimated to be approximately 5.0 nm in size. At the 20.0 at.% Ag^+ loading, the size of the silver deposits were estimated to be 2.0 nm [22]. However, larger Ag deposits, and in some cases larger than the individual TiO_2 particles themselves (up to 125.0 nm in size) were also present. Therefore, as more and more silver ions are reduced, the silver deposits grow with increasing Ag^+ loadings. The large silver deposits are clearly seen in the TEM maps of Fig. 2. The Ag agglomerates produced at the 20.0 at.% Ag^+ loading could shield the TiO_2 surface, hindering light absorption and electron–hole pair generation. More Ag particles were present on the TiO_2 surface at this high metal loading than at the 2.0 at.% Ag^+ loading. At the 2.0 at.% Ag^+ loading, silver particles were only observed on some titania particles. However, at the 20.0 at.% Ag^+ loading, almost all TiO_2 particles were covered with small Ag particles [22]. The increased probability of hole capture by the larger number of silver deposits on 20.0 at.% Ag^+-modified TiO_2 particles decreases the probability of adsorbed organic molecules capturing holes. This could explain the lower activity of these particles compared to 2.0 at.% Ag^+-modified TiO_2 particles.

Herrmann et al. [6] have proposed a mechanism describing the deposition and growth of silver particles on the titania surface. Silver ions are initially adsorbed on the surface of TiO_2 particles. Electrons reduce adsorbed Ag^+ ions to silver metal atoms. The formation of small crystallites of silver can occur either by the agglomeration of silver atoms or by a cathodic-like successive reduction process. The agglomeration of silver atoms is described by

$$m\mathrm{Ag}^0 \rightarrow \mathrm{Ag}_m \tag{24}$$

The successive reduction sequence is represented by Eq. (25).

$$\begin{aligned}\mathrm{Ag}^0 + \mathrm{Ag}^+ &\rightarrow (\mathrm{Ag})_2{}^+ + \mathrm{e}^- \rightarrow \mathrm{Ag}_2 + \mathrm{Ag}^+ \rightarrow (\mathrm{Ag}_3)^+ \\ &+ \mathrm{e}^- \rightarrow \mathrm{Ag}_3 \rightarrow \cdots \rightarrow \mathrm{Ag}_m\end{aligned} \tag{25}$$

The basis for the above sequence is that since metal crystallites are enriched in photoproduced electrons, they can constitute sites for the cathodic-like reduction of cations, which would progressively increase the size of the metal deposit [6].

To determine the dependence of modified photocatalyst catalyst activity on substrate concentration, the photooxidation of 100 μg C (5.0 ppm C) sucrose (used to represent a low carbon loading) was performed using pure TiO_2 and silver-modified TiO_2 suspensions prepared at the 0.5, 2.0 and 20.0 at.% Ag^+ loadings. The results obtained are shown in Fig. 6.

The addition of silver ions into the suspension was of no effect. Although silver deposits were formed on the TiO_2 surface for all the Ag^+ loadings used there was no evident enhancement in the oxidation rate. The ratios of the instantaneous maximum oxidation rates of 0.5, 2.0 and 20.0 at.%

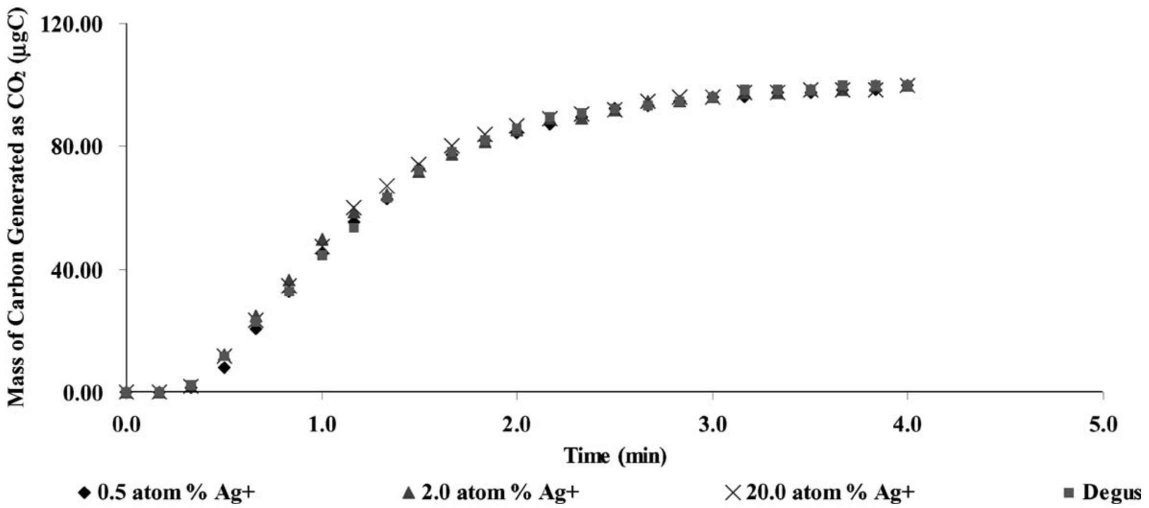

Fig. 6. Oxidation of 100 μg C sucrose using pure Degussa P25 and silver-modified Degussa P25 suspensions to determine the effect of organic loading on photocatalyst activity.

Ag^+-modified TiO_2 catalysts to pure TiO_2 were 1.06:1, 1.13:1 and 1.05:1, respectively, illustrating the almost identical behaviour of modified and bare catalysts. However, other experiments showed that modified TiO_2 suspensions performed better than pure TiO_2 suspensions for the oxidation of 250 and 450 μg C sucrose, even at the 0.5 at.% Ag^+ loading (not shown).

As mentioned earlier, the presence of silver deposits reduce electron–hole recombination thereby increasing the concentration of oxidising agents available for organic degradation and mineralisation. The rate of organic oxidation is dependent on the concentration of organic molecules and oxidising agents in the suspension. The rate equation describing the disappearance of the organic (C) can be written as

$$-\frac{\mathrm{d}C}{\mathrm{d}t} = k_{\mathrm{reaction}}[R][C] \qquad (26)$$

where $[R]$ is the concentration of the oxidising agents, $[C]$ the concentration of the organic substrate and k_{reaction} the rate constant [30]. For low organic loadings, the concentration of oxidising agents in titanium dioxide suspensions is in excess of the organic concentration. Thus any increase in $[R]$ by silver-modification of the particles will not significantly affect the reaction rate. On the other hand, at high organic loadings, the concentration of organic is in excess of the concentration of oxidising agents available. Increases in the concentration of oxidising agents by surface modification of titania particles is beneficial in this case. Hence the enhancement in the rate of reaction for high sucrose loadings is evident. Thus an appreciable concentration of substrate molecules should be available in the modified suspension to take full advantage of the added possibility of hole capture [27].

3.3. Photooxidation of salicylic acid using bare and silver ion-modified titanium dioxide suspensions

The mineralisation and degradation of salicylic acid was conducted under an air-equilibrated environment using TiO_2 particles with and without silver metal surface modification. Salicylic acid absorbs UV–visible light best at a wavelength of 294 nm. The addition of salicylic acid to TiO_2 suspensions turns the colloid to yellow, indicating the formation of a titanium(IV)–salicylate charge transfer complex [31]. This was clearly visible for additions of high amounts of salicylic acid (2000 μg C).

The degradation and mineralisation of salicylic acid was monitored by quantifying the amount of salicylic acid remaining in solution and by measuring the amount of carbon dioxide generated after illumination for a certain period of time, respectively. The initial pH of the suspensions was adjusted to a value between 3.0 and 3.5. During the photooxidation of salicylic acid (100 and 2000 μg C) in the presence of silver ions (2.0 at.% Ag^+ loading), TiO_2 particles changed from white to light brown.

The mineralisation profiles of 2000 μg C salicylic acid obtained for TiO_2 and Ag/TiO_2 (2.0 at.% Ag^+) particles were identical (Fig. 7). Modification of TiO_2 particles with silver deposits does not enhance the mineralisation of 2000 μg C salicylic acid, which is in contrast to the results obtained for the mineralisation of 2000 μg C sucrose. A similar result was obtained for the mineralisation of 100 μg C salicylic acid. The photooxidation reaction of 2000 μg C salicylic acid was performed in another experiment where silver ions were deposited onto the titania surface before adding salicylic acid into the suspension. Again, the oxidation profiles for the pure TiO_2 and Ag/TiO_2 systems were identical to the plot obtained when adding silver ions and salicylic acid into the suspension simultaneously. This confirmed that the presence

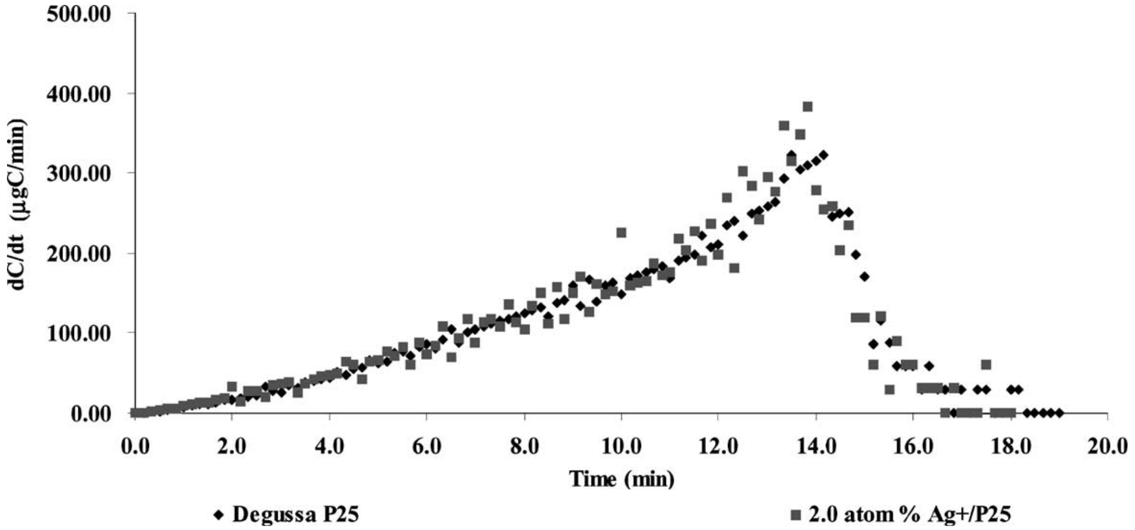

Fig. 7. Photooxidation of 2000 μg C salicylic acid using pure and 2.0 at.% Ag^+-modified Degussa P25 suspensions at pH 3.0.

of silver deposits on the TiO_2 surface were not able to enhance the mineralisation of salicylic acid. The contrasting results obtained for sucrose and salicylic acid mineralisation illustrate that the role of silver-modified TiO_2 particles in photocatalytic reactions is dependent on the type of organic compound involved in the reaction.

The pH of the pure Degussa P25 suspensions was unchanged after the mineralisation of 100 μg C salicylic acid (initial pH 3.5) but increased after the mineralisation of 2000 μg C salicylic acid from 3.0 to 3.6. In the presence of silver ions, a reduction in the suspension pH from 3.5 to 3.2 was observed after the photooxidation of 100 μg C salicylic acid. This reduction in pH is attributed to the oxidation of water by holes to H^+ ions and oxygen which occurs during the reduction of Ag^+ to Ag^0. A decrease in the suspension pH was not observed after the mineralisation of 2000 μg C salicylic acid since any decrease in pH due to Ag^+ reduction would have been masked by the increase in pH due to the mineralisation of 2000 μg C salicylic acid (initial pH 3.0, final pH 3.3).

The amount of silver deposited during the simultaneous reduction of silver ions and oxidation of salicylic acid was quantified by ICP-AES to be 48.8% (mass basis) at the 2.0 at.% Ag^+ loading. The amount of silver deposited during salicylic acid mineralisation was approximately the same as the amount deposited when using sucrose as the organic compound (2.0 at.% Ag^+ loading).

The oxidation profiles of salicylic acid in Fig. 8 are plots of the instantaneous oxidation rate versus illumination time for various salicylic acid loadings. The magnitude of the maximum instantaneous oxidation rate increases with increasing salicylic acid concentration. Similar observations were made for the photooxidation of various sucrose loadings. Comparison of the instantaneous oxidation rate of carbon versus time plots for sucrose and salicylic acid in the 100–2000 μg range of carbon loadings shows some noticeable differences. Firstly, Figs. 3, 4 and 8 show that the shape of the oxidation profiles change as sucrose and salicylic acid loadings greater than 100 μg C are oxidised. The rate profiles for high sucrose loadings (2000 μg C) can be divided into two sections. In the first section, the instantaneous oxidation rate rises very slowly. In the second section, or the latter part of the reaction, the instantaneous rate of oxidation rises rapidly before gradually decreasing to zero, at which point, the reaction has been completed.

However, for the Ag/TiO_2 system, the instantaneous oxidation rate profiles obtained for the degradation of 2000 μg C sucrose are similar in shape to the profiles obtained when using pure TiO_2 particles for the photooxidation of sucrose loadings of 100 μg C or less. This was also observed when a 2.0 at.% Ag^+-modified TiO_2 suspension was used for the mineralisation of 10,000 μg C sucrose. Similarly for 2000 μg C salicylic acid, the instantaneous oxidation rate rises with increasing illumination time until reaching a maximum value and then rapidly decreasing to zero, at which time the reaction is complete. Changes in the shape of the oxidation profile are seen for increasing loadings of salicylic acid. The time at which the maximum instantaneous oxidation rate occurs shifts towards the latter part of the reaction as the carbon loading is increased. The exception in the case of salicylic acid is that the oxidation profiles obtained when using Ag/TiO_2 and pure TiO_2 particles are similar for both low and high salicylic acid loadings. Also, the shape of the oxidation profiles obtained for sucrose and salicylic acid are different for high carbon loadings but similar for low carbon loadings.

The changes in the shapes of the oxidation profiles for sucrose and salicylic acid oxidation may be related to the formation of intermediate products during the reaction. The intermediate products of sucrose and glucose oxidation have been identified in other studies. The methods of oxidation used in these studies were not photocatalytic, but rather,

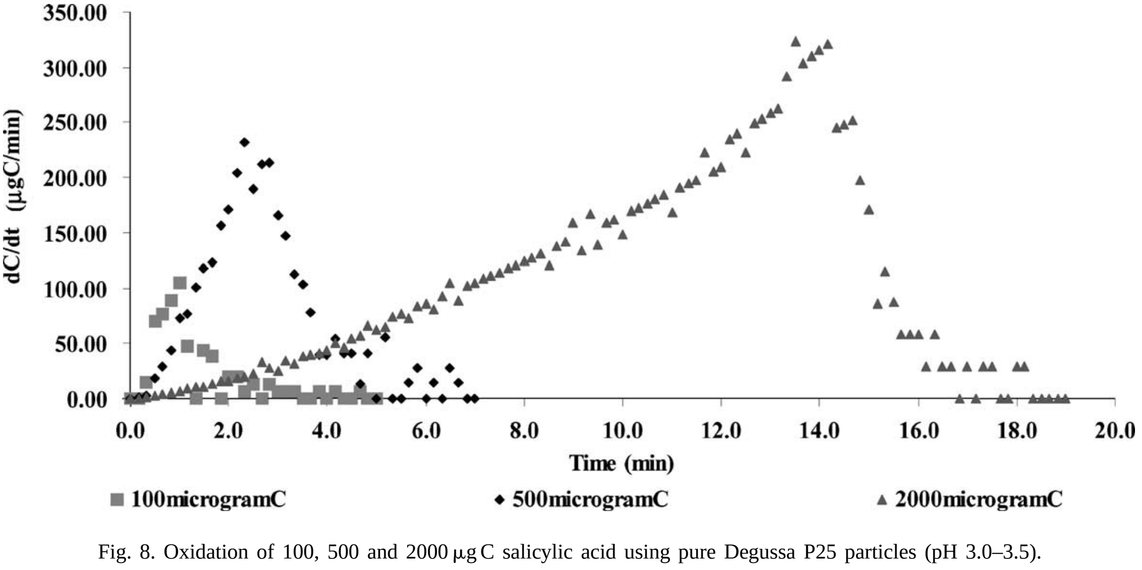

Fig. 8. Oxidation of 100, 500 and 2000 μg C salicylic acid using pure Degussa P25 particles (pH 3.0–3.5).

techniques such as electrocatalytic oxidation, electrochemical incineration, and wet oxidation were used. The main intermediate products of sucrose electrocatalytic oxidation have been identified as glucose, fructose, 2-keto-gluconic acid and glucuronic acid [32]. Other oxidation products of sucrose and glucose include a variety of carboxylic acids such as formic acid, glyceric acid, oxalic acid, lactic acid and acetic acid [33]. It has also been reported that glucose and its oxidised derivatives are tightly bound to the surface of platinised TiO_2 particles where they are eventually oxidised to CO_2 by the photo-Kolbe decarboxylation reaction [34]. The intermediate products of salicylic acid degradation, which require further oxidation to decompose to CO_2, have been identified as catechol and a mixture of dihydroxybenzoic acids (DHBAs). Catechol is formed by a photo-Kolbe type decarboxylation reaction and DHBAs by hydroxyl radical addition [35]. The prompt evolution of CO_2 during salicylic acid mineralisation indicates that other unstable intermediates are formed which are rapidly mineralised to CO_2 [35].

With increasing loadings of sucrose and salicylic acid, the concentration of intermediates produced during the reaction also increases. These intermediates require oxidative attack to degrade to simpler intermediates, which can be easily mineralised to CO_2. In modified titanium dioxide suspensions, due to the lower extent of electron–hole recombination, a higher amount of oxidising agents are available for organic degradation and mineralisation, compared to unmodified suspensions. For increasingly higher sucrose loadings, greater accumulation of intermediates occurs on the TiO_2 surface than on the Ag/TiO_2 surface. This is because less oxidising agents are available in the pure TiO_2 system, and hence the rate of intermediate degradation and mineralisation to CO_2 is slower than the rate of intermediate accumulation. The oxidation rate rises gradually in the pure TiO_2 system as more and more intermediates are degraded to simpler intermediates, which can be directly oxidised to the final product, CO_2. This last step of the reaction occurs rapidly, which is reflected by the steep increase in the instantaneous oxidation rate towards the latter part of the reaction. The differences in the shape of the oxidation profiles for high loadings of sucrose and salicylic acid are possibly due to the different nature of the intermediates formed, which require varying degrees of oxidation before mineralisation to carbon dioxide.

Although the mineralisation of salicylic acid was not enhanced when using Ag/TiO_2 particles as the photocatalyst, a series of experiments were conducted in which the photocatalytic degradation of salicylic acid was monitored instead. The purpose of these experiments was to determine whether the presence of silver deposits on the titania surface would enhance the degradation of salicylic acid even though the rate of salicylic acid mineralisation was unaffected. Fig. 9 shows changes in the concentration of salicylic acid molecules remaining in the suspension (SA), intermediate products remaining in the suspension+intermediates products adsorbed on the photocatalyst + salicylic acid molecules adsorbed on the photocatalyst $(I + I' + SA')$ and carbon dioxide (CO_2) generated as a function of illumination time. The data in Fig. 9 was obtained using the following method. The amount of salicylic acid remaining in solution was determined by UV–visible absorbance measurements, the amount of carbon dioxide generated by conductivity measurements and $(I+I'+SA')$ was obtained by subtracting $(SA+CO_2)$ from the initial amount of salicylic acid added to the suspension (2000 μg C in 20 ml).

Initially (illumination time = 0 min) the mass of salicylic acid measured in the suspension was much less than 2000 μg C. This was because approximately 65% of the

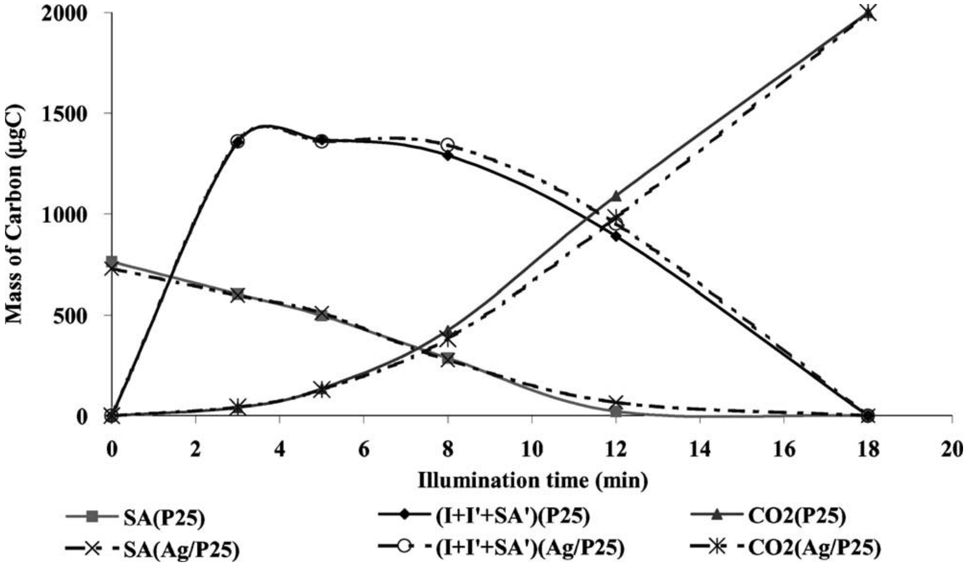

Fig. 9. Degradation of salicylic acid using pure and 2.0 at.% Ag^+-modified Degussa P25 suspensions at pH 3.0.

initial mass of salicylic acid added to the suspension had been adsorbed onto the photocatalyst particles in the absence and presence of silver ions (2.0 at.% Ag^+).

For both pure Degussa P25 suspensions and 2.0 at.% Ag^+-modified Degussa P25 suspensions, the degradation profiles were identical. This showed that in the case of salicylic acid, neither the degradation rate or the mineralisation rate is enhanced as a result of silver metallisation of TiO_2 particles. Carbon dioxide was evolved as soon as the suspensions were illuminated, while the concentration of salicylic acid decreased. The mass of intermediate products remaining in the suspension + intermediates products adsorbed on the photocatalyst + salicylic acid molecules adsorbed on the photocatalyst ($I + I' + SA'$) reached a maximum value of approximately 1500 μg C after illumination of the suspension for approximately 4 min.

The photocatalytic degradation of salicylic acid has been reported in previous publications using pure TiO_2 and modified TiO_2 particles and films as the photocatalyst. Lee et al. [7] reported that Ag/TiO_2 films exhibited enhanced activity for the decomposition of salicylic acid. Ag/TiO_2 films were 33% more active than pure TiO_2 films. Suri et al. [36], reported that platinised Aldrich and Degussa TiO_2 samples (1.0 and 0.5 wt.% Pt loadings, respectively) showed enhanced activities for degradation of salicylic acid. The experiments were performed at an initial pH of 4, at which the maximum adsorption of salicylic acid molecules on TiO_2 particles occurred. Prairie et al. [37], studied the photodegradation of salicylic acid during the simultaneous reduction of a variety of metals ions. The addition of metal ions to the system improved the rate of salicylic acid oxidation. In the presence of O_2, fairly rapid degradation of salicylic acid was observed. In the absence of O_2, the degradation of salicylic acid occurred for Pt^{4+}, Hg^{2+}, Au^{3+} and Ag^+ ions. They found that for the degradation of salicylic acid to occur in an O_2-free environment, the reduction of metal ions must occur until all organic is consumed (Ag^+, Hg^{2+}). It was concluded that the oxidation of salicylic acid was controlled by the rate of reduction or by the rate at which electrons are withdrawn from the conduction band of the photocatalyst. When reduction is slow, most electrons and holes simply recombine.

Other publications have previously mentioned that surface modification of TiO_2 particles either decreases catalyst activity or has no effect. Suri et al. [36], state that the surface and physicochemical properties of the TiO_2 sample used for modification with metal deposits affects the activity of the resulting modified photocatalyst. An enhancement in the rate of trichloroethylene destruction was observed when using platinised Aldrich TiO_2, whereas a detrimental effect occurred with platinised Degussa TiO_2 particles. This may be related to interactions occurring between the metal deposit and TiO_2 particles. Chlorobenzoic acid was found to adsorb strongly to the surface of Degussa P25 TiO_2 with the carboxylic group linked to the surface in interaction with the hydroxyl sites of titania. A deposit of 1.0 wt.% Pt on TiO_2 particles, prepared by the incipient wetness impregnation method decreased the activity of TiO_2 particles by a factor of 2.5 for the mineralisation of chlorobenzoic acid to CO_2 [38]. The decrease in activity is due to electron transfer from the support to the metal deposit, which was detrimental to the oxygen ionosorption $O_2{}^-$ species of titania. The addition of $AgNO_3$ to TiO_2 suspensions resulted in an inhibition of dichloroacetic acid (DCA) degradation [8]. The inhibiting effect is thought to be caused by the formation of H_2O_2 in the system due to the generation of additional protons. Hydrogen peroxide can undergo reduction as well as oxidation (Eqs. (19) and (20)). The oxidation of H_2O_2 consumes oxidising species required by organics. Lindner et al. [8], also suggest that it is possible that Ag^+ ions are oxidised to Ag^{2+}, due to the high oxidation potential of holes in TiO_2. Platinisation of the photocatalyst or the addition of Cu^{2+} ions into the suspension was beneficial for DCA degradation whereas these modifications were of no effect for the degradation of 4-chlorophenol. Copper ions and especially platinum deposits can also act as catalysts for reductive processes, such as the reduction of oxygen species by electrons. It is proposed that for DCA, the rate of oxygen reduction is rate-limiting whereas for 4-chlorophenol degradation the rate-limiting step is the attack of organic molecules by holes or hydroxyl radicals. Thus, the type of organic compound used in the photocatalytic reaction determines the performance of the modified photocatalyst. Similarly, in this study, it is proposed that the rate of sucrose mineralisation is enhanced in the presence of silver-modified TiO_2 particles since the rate-limiting step in this reaction is the transfer of electrons to dissolved oxygen molecules. In the case of salicylic acid degradation and mineralisation, the rate-limiting step is the reaction of holes and hydroxyl radicals with salicylic acid molecules and its degradation intermediate products [8]. However, further experiments are required to verify these postulations and efforts in this direction are currently being undertaken.

4. Conclusions

The photocatalytic oxidation of sucrose and salicylic acid to carbon dioxide and water was performed at pH 3.0–3.5 using bare and silver-modified TiO_2 particles. An optimum metal ion loading of 2.0 at.% Ag^+ was observed at which the most efficient photocatalyst was generated. The presence of nanosize metallic silver particles on the titania surface was found to enhance the activity of TiO_2 by a factor of 4.0 for the mineralisation of sucrose but had negligible effect on the degradation and mineralisation of salicylic acid.

Silver deposits on the TiO_2 surface behave as sites where electrons accumulate. Better separation of electrons and holes on the modified TiO_2 surface, allows more efficient channelling of the charge carriers into useful reduction and oxidation reactions rather than recombination reactions.

The performance of metallised TiO_2 particles is a function of the type of organic compound used in the reaction. The rate-limiting step in the mineralisation of sucrose is believed to be the transfer of electrons to dissolved oxygen species. Therefore, the enhanced mineralisation of sucrose is due to the more efficient reduction of dissolved oxygen molecules to superoxide radicals on the Ag/TiO_2 surface. Superoxide radicals are necessary for the formation of hydroxyl radicals or for reaction with organic radicals, which may be involved in the mineralisation of sucrose. In the case of salicylic acid degradation and mineralisation, the rate-limiting step is proposed to be the reaction of holes and hydroxyl radicals with organic molecules.

Acknowledgements

V. Vamathevan would like to thank the Australian Federal Government for financial assistance provided through the Australian Postgraduate Award (APA) program.

References

[1] J.C. Crittenden, J. Liu, D.W. Hand, D.L. Perram, Water Res. 31 (1997) 429.

[2] H. Tada, K. Teranishi, Y.-I. Inubushi, S. Ito, Chem. Commun. 21 (1998) 2345.

[3] A. Sclafani, J.-M. Herrmann, J. Photochem. Photobiol. A 113 (1998) 181.

[4] S.-I. Nishimoto, B. Ohtani, H. Kajiwara, T. Kagiya, J. Chem. Soc., Faraday Trans. 1 79 (1983) 2685.

[5] A. Sclafani, M.-N. Mozzanega, P. Pichat, J. Photochem. Photobiol. A 59 (1991) 181.

[6] J.-M. Herrmann, J. Disdier, P. Pichat, J. Catal. 113 (1988) 72.

[7] W. Lee, H.-S. Shen, K. Dwight, A. Wold, J. Solid State Chem. 106 (1993) 288.

[8] M. Lindner, J. Theurich, D.W. Bahnemann, Water Sci. Technol. 35 (1997) 79.

[9] J. Disdier, J.-M. Herrmann, P. Pichat, J. Chem. Soc., Faraday Trans. I 79 (1983) 651.

[10] J.-M. Herrmann, J. Disdier, P. Pichat, J. Phys. Chem. 90 (1986) 6028.

[11] E. Borgarello, N. Serpone, G. Emo, R. Harris, E. Pelizzetti, C. Minero, Inorg. Chem. 25 (1986) 4499.

[12] J. Papp, H.-S. Shen, R. Kershaw, K. Dwight, A. Wold, Chem. Mater. 5 (1993) 284.

[13] M. Albert, Y.-M. Gao, D. Toft, K. Dwight, A. Wold, Mater. Res. Bull. 27 (1992) 961.

[14] Y.-M. Gao, W. Lee, R. Trehan, R. Kershaw, K. Dwight, A. Wold, Mater. Res. Bull. 26 (1991) 1247.

[15] W.-Y. Lin, K. Rajeshwar, J. Electrochem. Soc. 144 (1997) 2751.

[16] P. Pichat, in: M. Schiavello (Ed.), Photocatalysis and Environment: Trends and Applications, NATO Advanced Study Institute on New Trends and Applications, Kluwer Academic Publishers, Dordrecht; Boston, 1993, pp. 399.

[17] D.W. Bahnemann, M. Hilgendorff, R. Memming, J. Phys. Chem. B 101 (1997) 4265.

[18] N. Serpone, D. Lawless, J. Disdier, J.-M. Herrmann, Langmuir 10 (1994) 643.

[19] W. Choi, A. Termin, M.R. Hoffmann, J. Phys. Chem. 98 (1994) 13669.

[20] M. Abdullah, G.K.-C. Low, R.W. Matthews, J. Phys. Chem. 94 (1990) 6820.

[21] R.W. Matthews, J. Catal. 111 (1988) 264.

[22] V. Vamathevan, H. Tse, R. Amal, G. Low, S. McEvoy, Catal. Today 68 (2001) 201.

[23] G.K.-C. Low, S.R. McEvoy, S. Saricilar, A.M. Maitra, in: Proceedings of the Third National Hazardous and Solid Waste Convention, Sydney, 26–30 May 1996, pp. 711–718.

[24] I. Ilisz, Z. Laszlo, A. Dombi, Appl. Catal. A 180 (1999) 25.

[25] H. Tada, K. Teranishi, Y.-I. Inubushi, S. Ito, Langmuir 16 (2000) 3304.

[26] G. Yu, W. Zhu, Z. Yang, Z. Li, Chemosphere 36 (1998) 2673.

[27] M.R. Dhananjeyan, R. Annapoorani, R. Renganathan, J. Photochem. Photobiol. A 109 (1997) 147.

[28] H. Gerischer, A. Heller, J. Electrochem. Soc. 139 (1992) 113.

[29] M. Huang, E. Tso, A.K. Datye, M.R. Prairie, B.M. Stange, Environ. Sci. Technol. 30 (1996) 3084.

[30] M.T. Emett, Photochemical oxidation of arsenic(III) by oxygen and iron in acidic solutions, Ph.D. Thesis, October 1999.

[31] A.E. Regazzoni, P. Mandelbaum, M. Matsuyoshi, S. Schiller, S.A. Bilmes, M.A. Blesa, Langmuir 14 (1998) 868.

[32] P. Parpot, K.B. Kokoh, E.M. Belgsir, E.M.J.-M. Leger, B. Beden, C. Lamy, J. Appl. Electrochem. 27 (1997) 25.

[33] T.A. Patrick, M.A. Abraham, Environ. Sci. Technol. 34 (2000) 3480.

[34] M.R.St. John, A.J. Furgala, A.F. Sammells, J. Phys. Chem. 87 (1983) 801.

[35] A. Mills, C.E. Holland, R.H. Davies, D. Worsley, J. Photochem. Photobiol. A 83 (1994) 257.

[36] R.P.S. Suri, J. Liu, D.W. Hand, J.C. Crittenden, D.L. Perram, M.E. Mullins, Water Environ. Res. 65 (1993) 665.

[37] M.R. Prairie, L.R. Evans, B.M. Stange, S.L. Martinez, Environ. Sci. Technol. 27 (1993) 1776.

[38] H. Tahiri, Y. Ait Ichou, J.-M. Herrmann, J. Photochem. Photobiol. A 114 (1998) 219.